

Predictions for a planet just inside Fomalhaut’s eccentric ring

Alice C. Quillen

Department of Physics and Astronomy, University of Rochester, Rochester, NY 14627; aquillen@pas.rochester.edu

23 September 2018

ABSTRACT

We propose that the eccentricity and sharpness of the edge of Fomalhaut’s disk are due to a planet just interior to the ring edge. The collision timescale consistent with the disk opacity is long enough that spiral density waves cannot be driven near the planet. The ring edge is likely to be located at the boundary of a chaotic zone in the corotation region of the planet. We find that this zone can open a gap in a particle disk as long as the collision timescale exceeds the removal or ejection timescale in the zone. We use the slope measured from the ring edge surface brightness profile to place an upper limit on the planet mass. The removal timescale in the chaotic zone is used to estimate a lower limit. The ring edge has eccentricity caused by secular perturbations from the planet. These arguments imply that the planet has a mass between that of Neptune and that of Saturn, a semi-major axis of approximately 119 AU and longitude of periastron and eccentricity, 0.1, the same as that of the ring edge.

Key words: stars:individual:Fomalhaut; stars: planetary systems ; planetary systems : protoplanetary disks

1 INTRODUCTION

The nearby star Fomalhaut hosts a ring of circumstellar material (Aumann 1985; Gillett 1985) residing between 120 and 160 AU from the star (Holland et al. 1998; Dent et al. 2000; Holland et al. 2003). The ring is not axisymmetric. *Spitzer Space Telescope* infrared observations of Fomalhaut reveal a strong brightness asymmetry in the ring (Stapelfeldt et al. 2004; Marsh et al. 2005). Submillimeter observations are less asymmetric in brightness but also imply that the ring is offset, with the southern side nearer the star than the opposite side (Holland et al. 2003; Marsh et al. 2005). Recent *Hubble Space Telescope (HST)* observations show that this ring has both a steep and eccentric inner edge (Kalas et al. 2005). In this paper we explore dynamical scenarios involving a planet that can account for both the eccentricity of the ring edge and its sharp or steep surface brightness edge profile.

Two classes of theoretical models exist for non-transient eccentric rings that do not rely on dynamics induced by radiation pressure. These are the pericenter glow model (Wyatt et al. 1999) and the self-gravitating eccentric ring models (e.g., Goldreich & Tremaine 1979; Tremaine 2001; Papaloizou & Melita 2005). The self-gravitating ring models have primarily been used to explain eccentric planetary rings. Though the structure of the ring edge can impact the models (Chiang & Goldreich 2000), the ring edges are not integral to the model, instead the rings are truncated by torques driven by neighboring satellites.

The pericenter glow model can account for eccentricity in the disk surface brightness distribution of Fomalhaut’s disk (Stapelfeldt et al. 2004; Marsh et al. 2005). Secular perturbations from a planet interior to the ring cause particle eccentricities to be coupled with their longitudes of periastron. The forced particle eccentricities cause an asymmetry in the dust distribution such that the ring periastron is aligned with the planet’s periastron. Previous studies have not placed constraints on the location of the planet causing the forced eccentricity in Fomalhaut’s disk, consequently constraints on the planet’s mass and eccentricity are lacking (Wyatt et al. 1999; Marsh et al. 2005).

We briefly review the observed properties of Fomalhaut’s disk. The recent *HST* observations have revealed that the ring edge has eccentricity $e_{edge} = 0.11 \pm 0.01$, periastron at $PA = 170^\circ$, inclination 65.6° , and a semi-major axis $a_{edge} = 133$ AU (Kalas et al. 2005). The surface brightness at the edge drops by a factor of 2 within 10 AU (see Figure 3 by Kalas et al. 2005). This can be compared to the resolution of *HST*, $0.1''$, corresponding to only 0.75 AU at the distance of Fomalhaut. The slope of the disk edge was modeled with a disk scale height of 3.5AU corresponding to an opening angle of 1.5° (Kalas et al. 2005). However, the observed disk edge slope could either be due to the thickness of the disk or a drop in the planar surface density profile. Assuming an exponential dust density distribution in the form $\exp\left(-\frac{(a_{edge}-a)}{h_r} - \frac{|z|}{h_z}\right)$, the observed disk edge slope

2 Quillen

implies that either $h_r/r \sim 0.026$ and $2h_z < h_r$ or the disk aspect ratio $h_z/r \sim 0.013$ and $2h_z > h_r$. The equation of hydrostatic equilibrium can be used to place a limit on the velocity dispersion, u , of the dust particles, $\frac{u}{na} \lesssim 0.013$ where n is the mean motion at a semi-major axis a .

The age of the star is 200 ± 100 Myr (Barrado y Navascues 1998). The mass of the star is $2M_\odot$ (Song et al. 2001), so the rotation period at 130 AU is 1000 years. This orbital rotation period divided by the star's age is 10^5 . The optical depth (normal to the disk plane) just interior to the ring edge at $24\mu\text{m}$ is $\tau \sim 1.6 \times 10^{-3}$ (Marsh et al. 2005). The collision time in the ring, $t_{col} \sim (\tau n)^{-1}$, is a million years or 1000 orbits. Since this timescale is short, we can exclude Poynting-Robertson driven resonance capture models for the dust, as argued in detail by Wyatt (2005).

2 THE PERICENTER GLOW MODEL AND AN ECCENTRIC EDGE IN FOMALHAUT'S DISK

We follow the theory for secular perturbations induced by a planet (e.g., Murray & Dermott 1999; Wyatt et al. 1999). Secular perturbations in the plane can be described in terms of the complex eccentricity variable, $z = e \exp(i\varpi)$, where e is the object's eccentricity and ϖ is its longitude of periastron (e.g., Murray & Dermott 1999; Wyatt et al. 1999). The time variation of z is

$$\dot{z} = z_{forced} + z_{proper}(t) \quad (1)$$

where

$$z_{forced} = \frac{b_{3/2}^2(\alpha)}{b_{3/2}^1(\alpha)} e_p \exp(i\varpi_p) \quad (2)$$

(Murray & Dermott 1999; Wyatt et al. 1999). We denote the planet's semi-major axis, eccentricity and longitude of periastron as a_p , e_p , and ϖ_p , respectively. Here $\alpha = a_p/a$ if $a_p < a$ otherwise $\alpha = a/a_p$. The functions, $b_s^j(\alpha)$, are Laplace coefficients (see Murray & Dermott 1999 for definitions and numerical expressions). If the planet's periastron does not vary (as for the two body problem) then z_{forced} is a constant of motion. In this case the forced complex eccentricity depends only the planet's semi-major axis and eccentricity, and not on its mass.

The ratio of Laplace coefficients, $b_{3/2}^2(\alpha)/b_{3/2}^1(\alpha) < 1$, so the amplitude of the complex eccentricity variable, $|z_{forced}|$, cannot exceed the planet's eccentricity. If the planet is near the ring edge then α is near 1. Near the planet $\lim_{\alpha \rightarrow 1} [b_{3/2}^2(\alpha)/b_{3/2}^1(\alpha)] = 1$ and $|z_{forced}| = e_p$. If the planet is near the ring edge then the forced eccentricity is equal to that of the planet.

We now consider the density distribution from a distribution of particles. Particles with the same semi-major axis, different mean anomalies and zero free or proper eccentricities would be located along a single ellipse. If the free eccentricities are non zero then the density distribution is smoother than the zero free eccentricity ellipse and has a width twice the free eccentricity multiplied by the semi-major axis. Consequently the observed steepness of the disk edge limits the distribution of free eccentricities in the edge. We denote the free eccentricity dispersion, $u_e^2 = \langle e_{proper}^2 \rangle$.

The slope of Fomalhaut's disk edge $h_r/r \lesssim 0.026$ so the free eccentricities in the disk edge are $u_e \lesssim 0.026$. If the planet is responsible for truncating the disk and limiting the distribution of free eccentricities then we suspect that the planet is located near the disk edge and α is almost 1. If the ring eccentricity is due to secular perturbations from a planet then the hypothetical planet's eccentricity e_p is equal to that of the edge or $e_p \sim 0.11$.

Since they are inelastic, collisions damp the eccentricities and inclinations of an ensemble of particles. This damping leads to a distribution following nearly closed (non-self-intersecting) orbits. Near a planet the only non-intersecting closed orbits consist of those with zero free eccentricity and with eccentricity equal to the forced eccentricity.

3 SPIRAL DENSITY WAVES AND THE COLLISION TIMESCALE

In a high opacity, $\tau \sim 1$, disk spiral density waves are driven by a planet or satellite near the planet. A gap opens if the torque from the planet exceeds that from accretion and the minimum gap width is twice the size of the planet's Hill sphere (e.g., Borderies et al. 1989).

As pointed out two hundred years ago by Poisson, some form of interaction between particles is needed for secular transport to occur. Satellites or planets do not exert a torque on a collisionless disk. However, planetesimals in the corotation region are efficiently pumped to high eccentricity and ejected by the planet or other interior planets (e.g., David et al. 2003; Mudryk & Wu 2006). In this case the width of a gap opened near the planet would be given by Equation (5), as is discussed further in section 4. For planet mass objects the width of this chaotic zone exceeds that set by the Hill radius because $2/7$ is smaller than $1/3$.

The separation between collisional and collisionless disks is important as the opacity of the disk (setting the collision timescale) is an observable. Franklin et al. (1980); Goldreich & Tremaine (1980); Lissauer & Esprestate (1998) showed that spiral density waves were efficiently driven at a Lindblad resonance by a satellite when the collision timescale was above a critical one, t_{crit} , where $t_{crit} \propto \mu^{-2/3}$, and $\mu \equiv \frac{m_p}{M_*}$ is the ratio of the planet mass divided by that of the star. This has been confirmed numerically with simulations of low opacity collisional particle disks at individual Lindblad resonances (Franklin et al. 1980; Hanninen & Salo 1992; Esprestate & Lissauer 2001). Lissauer & Esprestate (1998) predicted this scaling by comparing the period of excited epicyclic oscillations at a Lindblad resonance with the collision timescale. Near a planet a series of resonances is encountered. The $j : j - 1$ mean motion resonance (corresponding to the $m = j - 1$ Lindblad resonance) has a period approximately equal to the renormalization factor in Equation (7) by Quillen (2006) or

$$p_e \sim n^{-1} |\delta_{1,0} a'|^{-2/3} = n^{-1} \left| \frac{3j^2 \mu \sqrt{2}}{2\pi da} \right|^{-2/3} \quad (3)$$

with coefficients described by this work, and evaluated above in the limit of large j . In the limit of small da , and setting the critical timescale to this period, $t_{crit} = p_e$,

$$t_{crit} n \sim \mu^{-2/3} j^{-2} \sim \mu^{-2/3} da^2. \quad (4)$$

We have recovered the scaling with planet mass predicted by previous works (Goldreich & Tremaine 1980; Franklin et al. 1980; Lissauer & Espresate 1998) but have also included a dependence on distance from the planet.

The above critical timescale, t_{crit} , (appropriate for small da) increases with distance from the planet. For a disk with a particular collision timescale, spiral density waves would be driven past a particular distance from the planet. Because the Hill sphere radius is proportional to the planet mass to the 1/3 power, Equation (4) implies that t_{crit} is of order 1 at the Hill sphere radius. Only collisional disks, $\tau \sim 1$, could have a disk edge extending to the planet's Hill sphere. Since the opacity of Fomalhaut's disk is sufficiently low that spiral density waves cannot be driven into the disk by a nearby planet, the disk edge must be maintained by a different dynamical process.

4 VELOCITY DISPERSION AT THE EDGE OF THE CHAOS ZONE

There is an abrupt change in dynamics as a function of semi-major axis at the boundary of the chaos zone in the corotation region near a planet. The width of this zone has been measured numerically and predicted theoretically for a planet in a circular orbit by predicting the semi-major axis at which the first order mean motion resonances overlap (Wisdom 1980; Duncan et al. 1989; Murray & Holman 1997; Mudryk & Wu 2006). The zone boundary is at

$$da_z \sim 1.3\mu^{2/7} \quad (5)$$

where da_z is the difference between the zone edge semi-major axis and that of the planet divided by the semi-major axis of the planet.

In section 2 we found that the free or proper eccentricities are likely to be limited by the observed disk edge slope. A collision could convert a planar motion to a vertical motion similar in size, suggesting that the disk velocity distribution is not highly anisotropic so we may assume $h_z/r \gtrsim u_e$. A collision could also increase or decrease the particle semi-major axis and eccentricity. Particle lifetime is likely to be strongly dependent on semi-major axis, so we expect a sharp boundary in the semi-major axis distribution. The slope in the disk edge is likely to be set by the vertical scale height and velocity dispersion in the disk edge. We estimate that $h_z/r \sim u_e \sim 0.013$. Here the value of 0.013 is half the scale height measured by Kalas et al. (2005) (see discussion at the end of section 2).

Outside the chaos zone, planetesimals still experience perturbations from the planet. These perturbations have a characteristic size set by size of perturbations in the nearest mean-motion resonance that is not wide enough to overlap others and so is not part of the chaotic zone. Since particles in the edge reside outside the chaotic zone, the velocity dispersion does not increase with time. Via numerical integration we find a relation, shown in Figure 1, between the planet mass and the proper eccentricity dispersion just outside the chaos zone. The numerical integrations were carried out in the plane, using massless and collisionless particles under the gravitational influence of only the star and a massive planet with eccentricity $e_p = 0.1$. The initial particle eccentricities were set to the forced eccentricity and the and

longitudes of periastron were chosen to be identical to that of the planet. Initial mean anomalies were randomly chosen. The free eccentricity distribution was measured after 10^5 planetary orbits. However u_e reached the steady state value much earlier in the integrations, at a time less a hundred planetary orbits and so shorter than the collision timescale.

The libration width for a $j : j - 1$ mean motion resonance has $e^2 \sim \mu^{2/3} j^{2/3}$ (using the high j limit of equation 7 by Quillen 2006). Setting $j \sim \mu^{-2/7}$ corresponding to the chaos zone boundary we estimate an eccentricity dispersion $u_e \sim \mu^{3/7}$ just outside the chaotic zone. This dependence on μ is shown as a solid line in Figure 1 and is a good match to the numerically measured dispersion values in the disk edge.

Fomalhaut's disk edge slope can be used to place a limit on the planet mass if we assume that the disk edge is bounded by the planet's chaotic zone. We use the limit, $u_e \sim 0.013$, based on the disk edge slope, shown as a horizontal line on Figure 1 to estimate the mass of the planet. This horizontal line is consistent with the eccentricity dispersion at the edge of a chaos zone for a planet of mass $\mu \sim 7 \times 10^{-5}$. As the mass of Fomalhaut is twice that of the Sun this corresponds to a planet mass similar to that of Neptune. For this simulation the distance between the planet semi-major axis and disk edge has $da \sim 0.13$, approximately consistent with the $\mu^{2/7}$ law and corresponding to a planet's semi-major axis of 119 AU.

If the velocity dispersion in the disk edge is due to perturbations from massive objects in the ring then it would exceed that estimated from our integrations. In this case the planet maintaining the disk edge could be lower, but not higher, than that estimated above. The mass ratio $\mu = 7 \times 10^{-5}$ can be regarded as an approximate upper limit for the planet mass.

5 REMOVAL TIMESCALE FROM THE COROTATION REGION

Since they are inelastic, collisions damp the eccentricities and inclinations of an ensemble, unless they are rapidly transported elsewhere. Since they change orbital parameters, collisions cause diffusive spreading of the particle distribution in an initially sharp ring edge. A particle that is knocked into an orbit with a semi-major axis within the chaotic zone can be scattered by the planet and ejected from the region. To maintain the low dust density within the ring edge, we infer that the removal timescale within the ring must be shorter than the rate that particles are placed interior to the ring.

We can approximate the dynamics with a diffusion equation where diffusion due to collisions in the disk edge is balanced by the rapid removal of particles on a timescale $t_{removal}$ inside the edge. In steady state the diffusion equation

$$\frac{\partial}{\partial a} \left(D \frac{\partial N}{\partial a} \right) \approx \frac{N}{t_{removal}} \quad (6)$$

(Melrose 1980; Varvoglis & Anastasiadis 1996), where $N(a)$ is the number density of particles with semi-major axis a . The diffusion coefficient, D , depends on the collision time and the velocity dispersion, u , in the disk, $D \sim \frac{u^2}{t_{col} n^2}$. This diffusion coefficient is similar to a viscosity and can be esti-

4 Quillen

mated by considering the mean free path and particle velocity differences set by the epicyclic amplitude. The removal timescale $t_{removal}$ is set by the dynamics within the chaos zone and depends on the planet mass and eccentricity. The above equation is satisfied when $N(a)$ decays exponentially with a scale length l , and $l^2 = Dt_{removal}$.

As the removal timescale depends on the planet mass and eccentricity it is useful to write

$$t_{removal} = l^2/D = \left(\frac{l}{h}\right)^2 t_{col} \quad (7)$$

In section 4 we argued that the velocity distribution is unlikely to be extremely anisotropic near the disk edge and that this dispersion is set by the planet and the distance to the disk edge. Therefore we expect that $l \sim h_z$. Equation (7) implies that in order for a planet to open a gap in a low opacity disk it must be massive and eccentric enough that the removal timescale in the chaos zone exceeds the collision timescale.

Previous works estimating ejection timescales in the corotation region have primarily concentrated on more massive mass ratios than $\mu = 10^{-4}$ (David et al. 2003; Mudryk & Wu 2006). Consequently we have estimated this timescale from numerical integrations. 100 particles were integrated in the plane with initial eccentricities and longitudes of periastron identical to those of the planet, random mean anomalies and differing initial semi-major axes. Particles were removed from the integration when their eccentricity was larger than 0.5. Figure 2 shows this removal timescale as a function of semi-major axis for planet mass ratios $\mu = 10^{-4}$, 2×10^{-5} and eccentricity $e_p = 0.1$. Figure 2 shows that the removal timescale in the chaotic zone for $\mu = 10^{-4}$ is similar or below to the estimated collision timescale for Fomalhaut, 10^3 orbits, whereas the removal timescale is longer than this time for $\mu \sim 2 \times 10^{-5}$. In section 4 we estimated that the planet mass must be lower than 7×10^{-5} . Here we find that if the planet mass is below $\mu \sim 2 \times 10^{-5}$ then the chaotic zone would not be able to open a gap in Fomalhaut's particle disk.

The diffusion equation (Equation 6) neglects any dependence of the diffusion coefficient or removal time on particle radius or eccentricity. We also have not considered the role of a particle size distribution and destructive collisions. The low scale height implied from the sharp edge implies that fewer collisions are destructive than previously estimated (e.g. by Wyatt & Dent 2002). A more sophisticated model is needed to more accurately predict the edge profile as a function of planet mass, eccentricity, collision timescale and particle size.

6 SUMMARY AND DISCUSSION

We find that a planet accounting for both the eccentricity and edge of Fomalhaut's disk is likely to have eccentricity similar to that of the disk edge or $e_p \sim 0.1$. Here we have assumed that the eccentricity of the ring is a forced eccentricity due to the planet. The sharp disk edge limits the free eccentricities in the ring edge, so the ring eccentricity equals the forced eccentricity. For a planet close enough to truncate the ring, the forced eccentricity is approximately the same as the planet eccentricity.

For high opacity or collisional disks ($\tau \sim 1$), a gap is only formed if the planet driven spiral density waves can overcome the torque from accretion. A planet just large enough to open a gap will open one approximately twice the size of its Hill radius. However, a collisionless disk can open a larger gap, the size of the chaos zone in the planet's corotation region. We find that spiral density waves can only be driven into a disk within a chaotic zone if the disk opacity is of order 1. Fomalhaut's disk opacity, $\tau \sim 1.6 \times 10^{-3}$ (Marsh et al. 2005), is sufficiently low that spiral density waves cannot be driven near the planet. For low opacity disks, $\tau \lesssim 0.1$, a planet will open a gap to the chaos zone boundary only if the collision timescale exceeds the timescale for removal of particles within the chaos zone. We use this limit and numerical integrations to infer that a mass of a planet sufficiently large to account for the sharp edge in Fomalhaut's disk edge has mass ratio $\mu \gtrsim 2 \times 10^{-5}$.

The planet mass can be estimated from the observed slope in the disk edge by assuming that the ring edge is located at the edge of the planet's chaos zone and the velocity dispersion at the ring edge is set by resonant perturbations caused by the planet. If the velocity dispersion estimated at the ring edge is due to perturbations caused by bodies in the ring then the planet mass must be lower than this estimate. This limits the planet mass ratio $\mu \lesssim 7 \times 10^{-5}$.

Our exploration suggests that there is a planet located just interior to Fomalhaut's ring with semi-major axis $\sim 119AU$, mass ratio $2 \times 10^{-5} \lesssim \mu \lesssim 7 \times 10^{-5}$ (corresponding to between a Neptune and Saturn mass), and longitude of periastron and eccentricity, $e_p \sim 0.1$, the same as that of the ring edge. Arguments similar to those explored here could be used to estimate the masses of bodies residing in and causing structure in other low opacity disks.

A Saturn mass at 119 AU may seem extreme compared to the properties of our Solar system (Neptune at 30 AU). It is desirable to place this predicted planet mass in context with the estimated mass of Fomalhaut's disk. The total mass required to replenish the dust in the disk was estimated by Wyatt & Dent (2002) to be $20 - 30M_{\oplus}$, however a larger mass is probably required since the velocity dispersion assumed by this study corresponded to $h/r \sim 0.1$ and this value exceeds by a factor of eight that consistent with the edge slope measured by Kalas et al. (2005); $h/r \sim 0.013$. A power law size distribution with an upper cutoff of 500 km leads to an estimate of 50-100 Earth masses in the ring (Kalas et al. 2005). These estimates suggest that there is sufficient material currently present in Fomalhaut's disk to form another Saturn or Neptune sized object.

We thank B. Zuckerman, R. Edgar, P. Kalas and E. Ford for interesting discussions. Support for this work was in part provided by National Science Foundation grant AST-0406823, and the National Aeronautics and Space Administration under Grant No. NNG04GM12G issued through the Origins of Solar Systems Program, and HST-AR-10972 to the Space Telescope Science Institute.

REFERENCES

- Aumann, H. H. 1985, PASP 97, 885
- Barrado y Navascues, D. 1998 A&A 339, 831

Borderies, N., Goldreich, P., & Tremaine S. 1989, *Icarus*, 80, 344
 Chiang, E. I. & Goldreich, P. 2000, *ApJ*, 540, 1084
 David, E.-M., Quintana, E.V., Fatuzzo, M., & Adams, F.C. 2003, *PASP*, 115, 825
 Dent, W. R. F., Walker, H. J., Holland, W. S., & Greaves, J. S. 2000, *MNRAS*, 314, 702
 Duncan, M., Quinn, T., & Tremaine, S. 1989, *Icarus*, 82, 402
 Espresate, J., & Lissauer, J. J. 2001, *Icarus*, 152, 29
 Franklin, F. A., Lecar, M., Lin, D. N. C., & Papaloizou, J. 1980, *Icarus*, 42, 271
 Gillett, F. 1985, in *Light on Dark Matter*, ed. F. P. Israel, (D. Reidel Co., Dordrecht), p. 61
 Goldreich, P., & Tremaine, S. 1979, *AJ*, 84, 1638
 Goldreich, P., & Tremaine, S. 1980, *ApJ*, 241, 425
 Hanninen, J., & Salo, H. 1992, *Icarus*, 97, 228
 Holland, W. S., et al. 2003, *ApJ*, 582, 1141
 Holland, W. S. et al. 1998, *Nature*, 392, 788
 Kalas, P., Graham, J. R., & Clampin, M. 2005, *Nature*, 435, 1067
 Lepage, I., & Duncan, M. J. 2004, *AJ*, 127, 1755
 Lissauer, J. J., Espresate, J. 1998, *Icarus*, 134, 155
 Marsh, K. A., Velusamy, T., Dowell, C. D., Grogan, K., & Beichman, C. A. 2005, *ApJ*, 620, L47
 Melrose, D. B. 1980, *Plasma Astrophysics*, Vol II (Gordon and Breach, New York)
 Mudryk, L. R., & Wu, Y. 2006, *ApJ*, 639, 423
 Murray, C. D. & Dermott, S. F. 1999, *Solar System Dynamics*, Cambridge University Press, Cambridge
 Murray, N., & Holman, M. 1997, *AJ*, 114, 1246
 Papaloizou, J.C.B., & Melita, M.D. 2005, *Icarus*, 175, 435
 Perryman, M.A.C., et al. 1997, *A&A*, 323, L49
 Quillen, A. C. 2006, *MNRAS*, 365, 1367
 Song, I., Caillault, J.-P., Barrado y Navascues, D., & Stauffer, J. R. 2001, *ApJ*, 546, 352
 Stapelfeldt, K. R., et al. 2004, *ApJS*, 154, 458
 Tremaine, S. 2001, *AJ*, 121, 1776
 Varvoglis, H., & Anastasiadis, A. 1996, *AJ*, 111, 1718
 Wisdom, J. 1980, *AJ*, 85, 1122
 Wyatt, M. C., & Dent, W. R. F. 2002, *MNRAS*, 334, 589
 Wyatt, M. C., Dermott, S. F., Telesco, C. M., Fisher, R. S., Grogan, K., Holmes, E. K., & Pina, R. K. 1999, *ApJ*, 527, 918
 Wyatt, M. C. 2005, *A&A*, 433, 1007

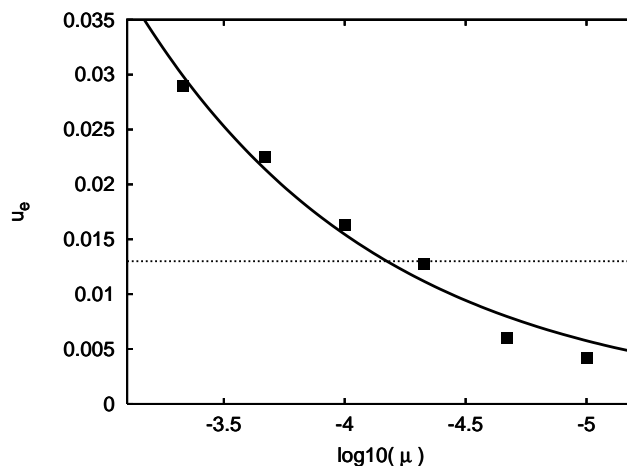


Figure 1. Eccentricity dispersion in the disk edge vs planet mass for a planet with eccentricity $e_p = 0.1$ (square points). The solid line is $u_e = 0.8\mu^{3/7}$. The scaling with $\mu^{3/7}$ is predicted for the libration in the first order mean motion resonance just outside the corotation region. The horizontal line shows the limit set from the observed disk edge slope.

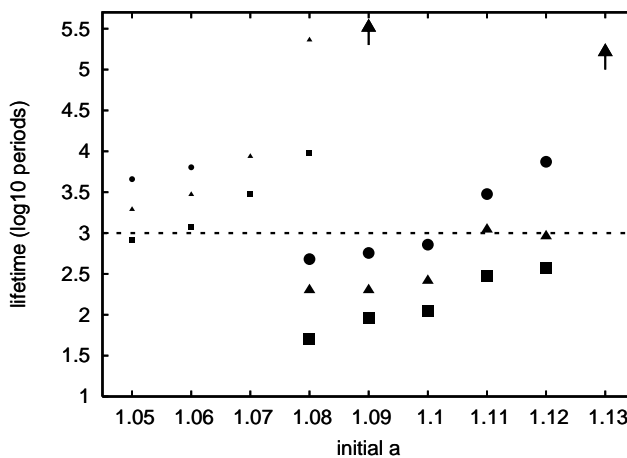


Figure 2. Removal timescale as a function of initial semi-major axis for a planet mass $\mu = 10^{-4}$ (large points) and $\mu = 2 \times 10^{-5}$ (small points). Particles were removed from the integration when their eccentricity became larger than 0.5. Squares, triangles and circles show the timescale when fewer than 75%, 50% and 25% of the particles remained in the integration, respectively. For an initial semi-major axis above or equal to 1.13, particles were not removed in less than 10^5 orbital periods (shown as the arrow on the upper right) for $\mu = 10^{-4}$ and for semi-major axis above or equal to 1.09 in less than 2×10^5 orbital periods for $\mu = 2 \times 10^{-5}$ (shown as the arrow on the top middle). The horizontal line shows the limit set from the collision timescale, 10^3 orbits, estimated from Fomalhaut's disk opacity. To account for the absence of dust within the ring edge, particle lifetimes within the chaotic zone must be shorter than the collision timescale.